

Extra-Column Band Spreading Concerns in Post-Column Photolysis Reactors for Microbore Liquid Chromatography

Arlen D. Kaufman, Ph.D.*
Peter T. Kissinger, Ph.D.
Purdue University
West Lafayette, IN 47907

*Corresponding author
Current address:
University of Evansville
Evansville, IN 47722

E-mail: ak2@evansville.edu

Minimization of extra-column volume in any LC method is crucial to maintaining the efficiency of the separation. This problem becomes even more challenging when working on the microbore scale. Nevertheless, it would be quite advantageous if existing post-column reaction technologies could be utilized with microbore LC in order to improve the detectability of a large variety of compounds that do not possess an easily detectable moiety. Post-column photolysis reactors, first reported by Iwaoka and Tannenbaum (1), are particularly intriguing in this regard because they provide a reagentless derivatization scheme and, consequently, do not require mixing the column effluent with any other flow streams. Even so, the volume of the reactor should be kept to a minimum, and the design should be one which will lead to as little extra-column band broadening as possible. With this problem in mind, several different designs of open-tubular reactors were studied in order to determine

Band spreading in coiled and straight tubes of circular cross-section was investigated as a function of flow rate in order to determine the optimal tubing geometry to utilize as a post-column reactor for microbore liquid chromatography (LC). The flow rates studied ranged from 0.030 to 1.2 mL/min, and three serpentine geometries and a helical coil geometry of various coil diameters were evaluated against a linear geometry. At the flow rates of the microbore experiment no distinct advantage in terms of band-spreading was observed between any of the serpentine geometries or the smallest diameter helical coil. However, using these geometries reduced the band spreading by up to 44 percent when compared to a linear tube of the same length.

their suitability to the scale and flow rates of microbore LC.

Band Spreading in Linear Open Tubes of Circular Cross Section

In an open-tubular reactor system, there is a trade-off between the residence time of an analyte in the reactor required for reaction and the band spreading associated with the analyte traversing the reactor. For a linear open-tubular reactor, the volumetric peak variance (σ_v^2) can be given by

$$\sigma_v^2 = \frac{\pi r_t^4 FL}{24D_m} \quad \text{EQ1}$$

where r_t is the radius of the tube, F is the volumetric flow rate, L is the length of the tube, and D_m is the molecular diffusion coefficient in the mobile phase. This equation is derived from Taylor's solution to dispersion of a non-compressible plug of fluid in a straight tube (2). It assumes that molecular diffusion along the longitudinal axis of the tubing is negligible, which is typi-

cally the case under most LC conditions. The residence time in a reactor (t_r) can be expressed by the following equation:

$$t_r = \frac{\pi r_t^2 L}{F} \quad \text{EQ2}$$

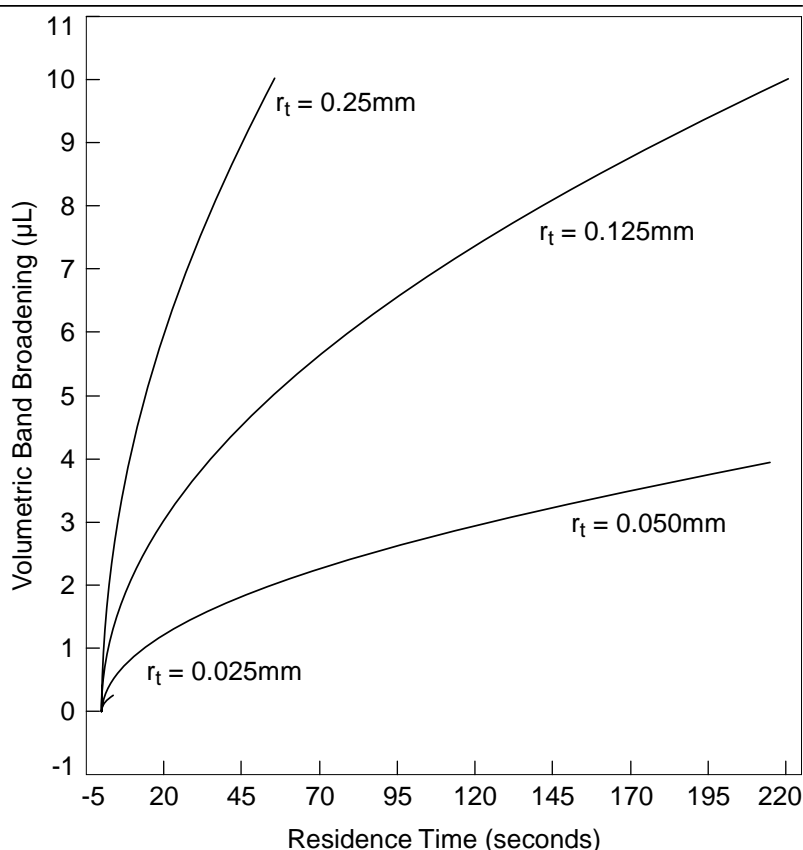
The peak variance as a function of the residence time can be obtained by combining **EQ1** and **EQ2** as shown below:

$$\sigma_v^2 = \frac{r_t^2 F^2 t_r}{24D_m} \quad \text{EQ3}$$

This equation predicts that in order to maximize residence time while minimizing the peak variance, it is best to use the smallest inner diameter tubing and the lowest flow rate allowable. However, these two variables are limited by the maximum allowable pressure drop across the reactor and the minimum chromatographic flow rate, respectively. **F1** illustrates extra-column band-broadening as a function of residence time for different reactor internal diameters. The flow rate in this case was chosen to be 50

F1

Volumetric band broadening in a straight open-tubular reactor as a function of residence time and tube radius. The maximum allowable pressure drop across the reactor was limited to 1000 psi, and the maximum band volume was held to 10 μL . The calculations were made at a flow rate of 50 $\mu\text{L}/\text{min}$.



$\mu\text{L}/\text{min}$, which is typically the practical low end of operation for a 1 mm x 10 cm column. The limiting values for the band-spreading curves in **F1** are either a peak volume of 10 μL , calculated as the full width at half maximum (FWHM), or a pressure drop associated with the reactor of 1000 psi (calculated from **EQ1**). This figure demonstrates the trade-offs between the tubing inner diameter and the residence time. In practice, the actual allowable variance and pressure drop may be larger or smaller depending on the experiment.

Band Spreading in Helically Coiled Tubes of Circular Cross Section

One method of decreasing the variance associated with flow in straight open tubing is to induce a secondary flow perpendicular to the parabolic laminar flow profile. This effect can be accomplished by simply coiling the tubing about its longitudinal axis. The secondary flow is generated by the centrifugal

forces acting on the moving fluid through a bend, and, since the axial velocity is greatest near the center of the tube, the fluid near the center is continuously being propelled towards the outer wall of the tubing. As a result, the fluid is forced to circulate in two vortices both above and below the central axis in order to replenish the fluid flow. Although this effect was first observed in the late 18th and early 19th centuries (3-8), the pioneering mathematical treatment of this phenomenon by Dean was not performed until 1927 (9-10).

Dean used perturbation analysis to solve the Navier-Stokes equation for fully developed flow of an incompressible Newtonian fluid in a curved pipe under the assumption that the coil diameter was large relative to the diameter of the tubing. The solution for the three-dimensional velocity profile is proportional to the dimensionless parameter duly named for its creator, the Dean number (Dn):

$$Dn = Re \sqrt{\frac{r_t}{r_c}} \quad \text{EQ4}$$

with r_c being the coil radius and Re the Reynolds number, given by

$$Re = \frac{8\rho F}{\pi r_t \eta} \quad \text{EQ5}$$

where ρ is the density of the fluid and η is the fluid's viscosity. The Dean number can be thought of as the ratio of the square root of the product of inertial and centrifugal forces to the viscous force.

Dean's solution to the velocity profiles of flow in coiled tubes has been shown to be valid only for a small range of Dean numbers ($Dn < 17$) due to the approximation that the curvature ratio ($\lambda = r_t/r_c$) must be small (11). As a result, a great deal of research has gone into extending the range of applicability of Dean's solution to larger Dean numbers. However, due to the complexity of the problem, no exact analytical solution exists to date.

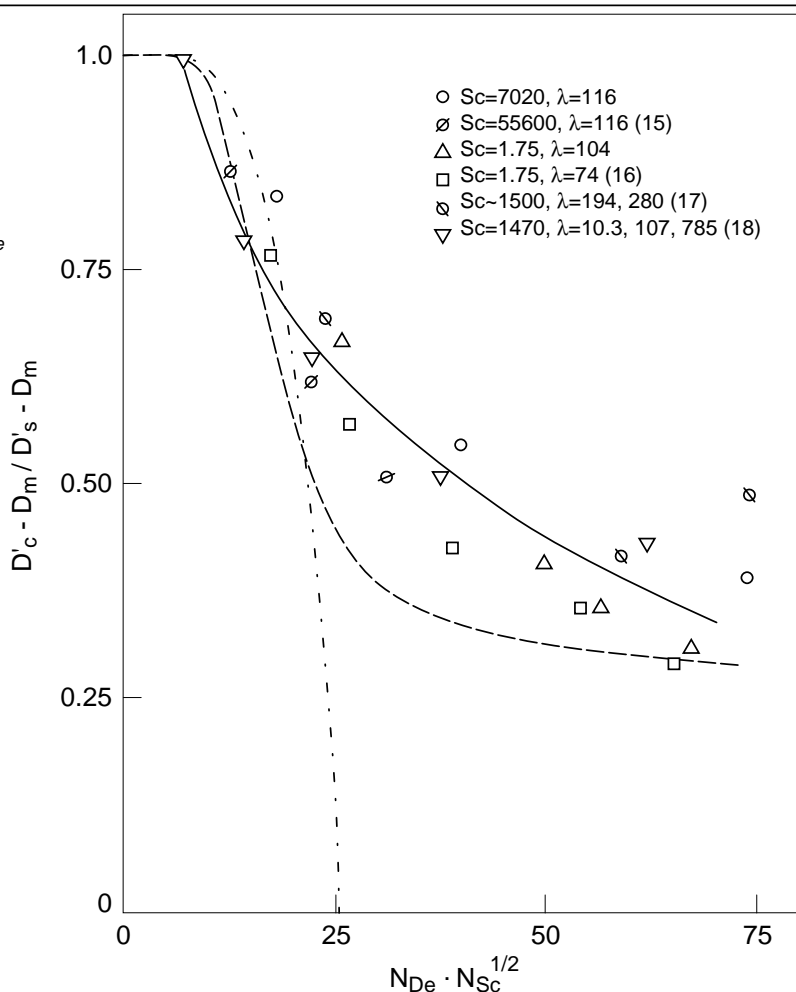
Even though Dean's analysis holds only for a small window of fluid flows, effective dispersion coefficients can be calculated from his velocity profiles by applying the Taylor (2) or Aris-Taylor (12) framework for dispersion theory. This approach was first attempted by Erdogan and Chatwin in 1967 (13), and their solution is expected to be valid over the range of applicability of Dean's solution ($Dn < 17$). The analysis was taken a step further by Janssen, who numerically solved the convective diffusion equations for diffusional effects combined with Dean's velocity profiles (14). An important outcome of this research was the finding that dispersion in coiled tubes can be correlated by the dimensionless parameter $Dn^2 Sc$, where Sc (the Schmidt number) is given by

$$Sc = \frac{\eta}{D_m \rho} \quad \text{EQ6}$$

Janssen found that for $Dn^2 Sc < 100$, no significant reduction in axial dispersion was observed compared with straight tubes. However, where

F2

Correlation of dispersion in coiled tubes. Theoretical analysis by Janssen (14) - - -; theoretical analysis by Erdogan and Chatwin (13) -.-.-; empirical correlation by Shetty and Vasudeva (15) ———. (Reprinted from reference 15, with kind permission from Elsevier Science Ltd.)



and straight tubes, respectively. The correlation obtained using this equation is shown in **F2** along with other theoretical models for dispersion in coiled tubes. Although there is a considerable amount of spread in the data, likely due to the large number of data sources, the empirical correlation fits quite well, especially when compared with the theoretical work of Janssen (14) and Erdogan, et al. (13).

Deelder, et al. (19) performed experiments over a larger range of $DnSc^{1/2}$ values and came up with their own empirical correlation for dispersion in coiled tubes:

$$\kappa = 1.52 - 0.275 \ln(DnSc^{1/2})$$

for $12.5 < DnSc^{1/2} < 200$, and

$$\kappa = 1$$

for $DnSc^{1/2} < 12.5$ **EQ8**

where $\kappa = D_c/D_s$, which assumes that the contribution from axial molecular diffusion is minimal in condensed phases. **F3** shows a plot of κ versus $DnSc^{1/2}$ for curvature ratios from 55 to 1024 over a range of Schmidt numbers from 180 to 380. This analysis extended the experimental correlation of dispersion in open tubes to $DnSc^{1/2} < 200$, although only a small range of Schmidt numbers were studied.

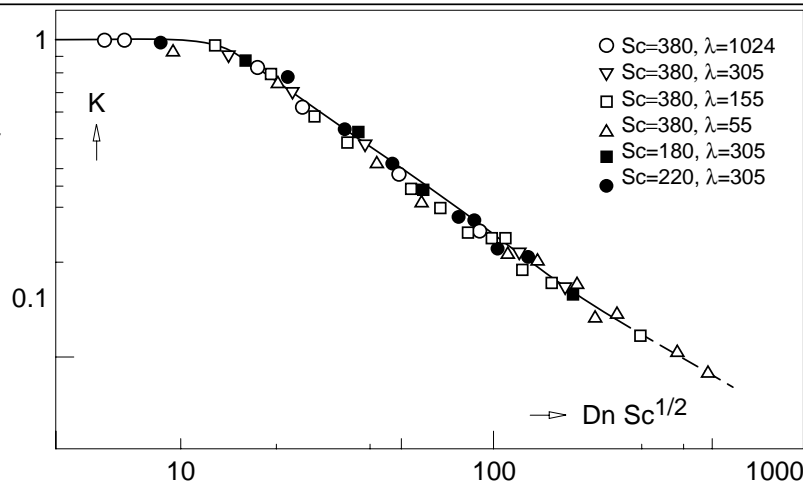
Iyer and Vasudeva (20) continued the analysis of Shetty, et al. (15) and extended the range of $DnSc^{1/2}$ to approximately 7000. Their new experimental correlation is represented by

$$\frac{D_c - D_m}{D_s - D_m} = 1.65 - 0.863 \log(DnSc^{1/2}) + 0.113 \log(DnSc^{1/2})^2$$

for $DnSc^{1/2} > 7$ and $\frac{D_c - D_m}{D_s - D_m} = 1$ for $DnSc^{1/2} < 7$ **EQ9**

F3

Correlation of dispersion in coiled tubes. Open symbols are nitrobenzene in isooctane; ■ benzene in chloroform; ● benzene in hexane. (Reprinted from reference 19, with kind permission from Elsevier Science—NL.)



$100 < Dn^2Sc < 5000$, axial dispersion was reduced by as much as two-thirds.

As a result of Janssen's discovery, other researchers have attempted to correlate their experimental results for dispersion in coiled tubes to the Dn^2Sc parameter. Shetty and Vasudeva (15) used the following empirical relationship

to correlate dispersion data for $DnSc^{1/2} < 75$:

$$\frac{D_c - D_m}{D_s - D_m} = 1.52 - 0.275 \ln(DnSc^{1/2})$$

for $DnSc^{1/2} > 7$, and

$$\frac{D_c - D_m}{D_s - D_m} = 1$$

for $DnSc^{1/2} < 7$ **EQ7**

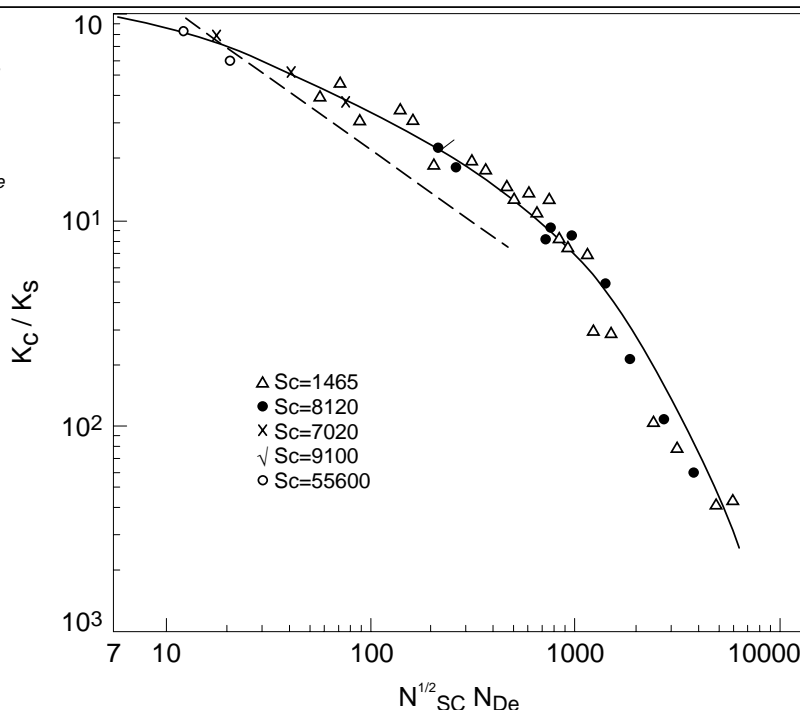
In these equations, D_c and D_s are the dispersion coefficients in coiled

F4 is a fit of this equation as well as the correlation obtained by Deelder, et al. (19) (**EQ8**). This new relationship was tested over a much larger range of Schmidt values (1465 to 55600), which may explain the discrepancies between it and Deelder's solution (19).

The previous three examples demonstrate the utility of correlat-

F4

Correlation of dispersion in coiled tubes. Empirical correlation by Iyer and Vasudeva (20) ———. Empirical correlation by Deelder, et al. (19) - - - - . (Reprinted from reference 20, with kind permission from Elsevier Science Ltd.)



ing the reduction in dispersion associated with coiled tubes to the dimensionless $DnSc^{1/2}$ parameter. However, no work has been done in the range of flow rates applicable to microbore chromatography. The following experimental evaluation attempts to rectify this problem by testing band spreading in open-tubular, helically coiled, and knitted reactors and comparing the results to the aforementioned solution.

Experimental

Solvent Delivery System

A Waters Associates (Milford, Mass.) model 590 programmable solvent delivery system module was used in conjunction with a flow splitter to provide flow rates above 200 $\mu\text{L}/\text{min}$. A piece of capillary tubing was used as the flow restriction device for the flow splitting system. The actual split flow rates were calculated by monitoring the time taken for the effluent to traverse a 50 μL glass disposable micropipet (Curtin Matheson Scientific, Inc., Houston, Tex.).

An sp210iw syringe pump from World Precision Instruments (Sarasota, Fla.) was used to provide flow rates below 200 $\mu\text{L}/\text{min}$. The

effluent was dispensed from the syringe pump by a 20 mL Micro-mate syringe from Popper and Sons, Inc. (New Hyde Park, NY). Flow rates were monitored in the same fashion as described earlier for flow rates above 200 $\mu\text{L}/\text{min}$.

A Rheodyne model 7520 injection valve (Rainin Instrument Company, Inc., Woburn, Mass.) with a 500 nL internal loop was used to introduce the sample onto each of the test reactors for both solvent delivery systems. This small volume injection system was chosen so that the injected sample volume would be negligible when compared to the final reactor dispersion volume.

Detection and Data Processing

Electrochemical detection was utilized to monitor the peak distributions coming off of the different reactor designs. A UniJet thin layer electrochemical flow cell from Bioanalytical Systems, Inc. (BAS) (West Lafayette, Ind.) with a 3 mm glassy carbon working electrode was chosen as the detection cell. This type of flow cell provides a very small detection volume, thereby minimizing the effects of the detector on the actual peak distribution of the test reactor. The po-

tential was applied to the UniJet with either a BAS LC-4C amperometric detector (for flow rates above 200 $\mu\text{L}/\text{min}$) or through the use of the electrochemical detector built into the BAS 200A LC system (for flow rates below 200 $\mu\text{L}/\text{min}$). The applied potential for all measurements was +600 mV versus the internal Ag/AgCl reference electrode of the UniJet cell. Data was collected from the LC-4C detector on a strip chart recorder and all peak distributions were analyzed manually to obtain peak widths and residence times. Data from the BAS 200A EC detector was collected digitally through the BAS 200A control software, and peak widths and residence times were determined automatically through the use of ChromGraph[®], a chromatographic data analysis program from BAS.

Test Reactors

All of the test open-tubular reactors were constructed out of one-meter lengths of 1/16" OD, 0.0229 cm ID Teflon tubing.

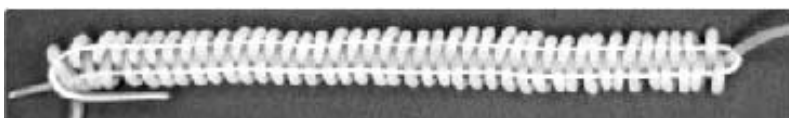
All linear reactors were stretched tightly between the injection valve and the detector cell in order to maintain as straight a reactor as possible.

Coiled helix reactors were made by tightly wrapping the reactor tubing around an appropriately sized piece of glass tubing. The same piece of reactor tubing that was used in the linear reactor was used for all of the coiled reactors, and the coils were constructed with the injector and the detection cell connected to the reactor throughout the study. This procedure was done in order to eliminate the problem of connectivity precision. Coils of the following curvature ratios were created: $\lambda = 442, 223, 123, 78.7, 39.4,$ and 10.0.

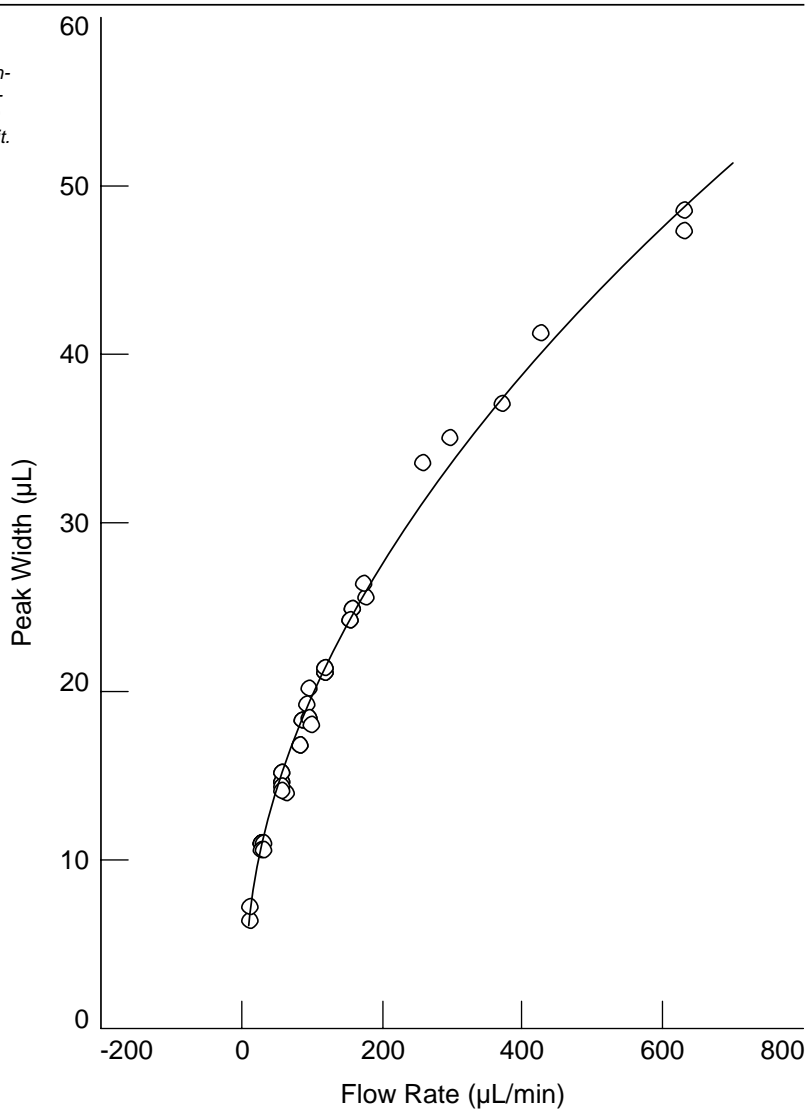
Knotted reactors were prepared by tying a linear array of overhand knots into the reactor tubing with the knots as close to one another as possible. This configuration is depicted in **F5A**.

F5

Photographs of the types of reactor being tested:
 A) knotted reactor design;
 B) knitted reactor design;
 C) figure-eight reactor design.

**A****B****C****F6**

Volumetric band spreading in a 1 m straight open-tubular reactor with an internal diameter of 0.0229 cm. ○ Raw data, — fit.



Knitted reactors were prepared using a special jig which consisted of eight pins (25 mm long and 2.4 mm in diameter), equally spaced in a circular arrangement with the diameter of the arrangement being 25 mm. The tubing was coiled in small loops around each pin in the jig, starting each loop from the inside of the jig, coiling around to the outside, and then back to the inside once again. This process was repeated until each of the pins had two loops around it. At that point, the lower of the two loops on each pin was pulled over the top of the upper loop and removed from the pin entirely. Then, a new single layer of tubing loops was added above the one remaining loop on each of the pins, and the process was repeated until the desired length of reactor was reached. A knitted reactor is shown in **F5B**. The size of the center of the reactor could be varied by changing the radius of the circle of pins, and the tightness of the weave could be controlled by the diameter of each individual pin and the number of pins used. In the actual jig employed to create the experimental reactors, eight pins were used, each with a diameter of 2.4 mm. The diameter of the circle of pins was 25 mm from pin center to pin center.

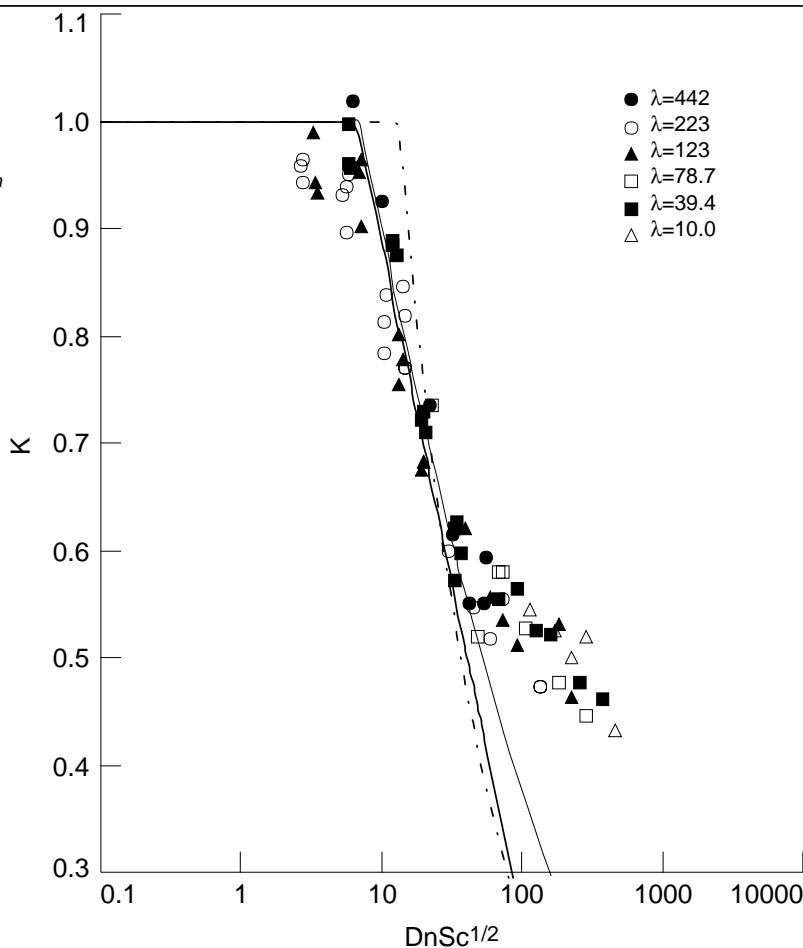
Tubing was coiled around two 2.0 mm diameter rods to create a stack of figure eights. **F5C** shows a diagram of this type of reactor.

Reagents

The buffer in which all of the experiments were performed was prepared by dissolving 13.8 g sodium phosphate monobasic, purchased from Aldrich Chemical Company, Inc. (Milwaukee, Wisc.), in 1.0 L of doubly distilled deionized water (Corning Megapure, Corning Incorporated, Corning, NY). The pH was then adjusted to 2.5 using HPLC grade 85% phosphoric acid (purchased from Fisher Scientific, Fair Lawn, NJ). To this solution, 5 mL of 1% (v:v) Pro-

F7

Correlation of dispersion in coiled tubes. Empirical correlation by Iyer and Vasudeva (20) - - - - . Empirical correlation by Deelder, et al. (20) - - - - . Empirical correlation by Shetty and Vasudeva (15) _____.



Clin150™:water (BAS part number CF-2150) was added as an antibacterial agent. The test solution used in all of the reactor experiments contained 966 nM gentisic acid (purchased from Sigma Chemical Company, St. Louis, Missouri) made up in the phosphate buffer previously described. This procedure was performed to ensure that the response observed was due to the gentisic acid alone and not a non-Faradaic response from the change in ionic strength of the injected plug.

Results and Discussion

To show the effects of coiling on dispersion in open tubes in the microbore regime, peak widths were monitored at flow rates from 0.030 to 1.2 mL/min. Since it is difficult to accurately measure flow rates at the lower end of this range, reported flow rates were calculated

from the ratio of the volume of the reactor to the peak residence time.

In order to be able to compare the reduction in dispersion in coiled reactors to that of a straight tube, band spreading in a straight tube of the same dimensions as the coiled tubes was measured as a function of flow rate. A plot of this data is shown in **F6**. The data was fit to Taylor's solution for dispersion from laminar flow in linear tubes (**EQ1**) (2). The molecular diffusion coefficient for the tracer compound was calculated from this fit as a measure of the validity of the data. The molecular diffusion coefficient for gentisic acid in the aqueous media was found to be 1.58×10^{-5} cm²/s, as expected.

The ratio of the dispersion in all of the reactors relative to the fit for dispersion in the straight tube, κ , was used as a marker for the efficiency of each reactor at minimizing band spreading. A plot of this

ratio as a function of $DnSc^{1/2}$ is shown in **F7** for all of the data from the helically coiled tubes. Curves corresponding to the empirical equations discussed earlier are also shown. None of the experimentally derived equations adequately fit the data as $DnSc^{1/2}$ becomes greater than approximately 30. This deviation may arise from the means in which the data was generated. In the previous experiments, large $DnSc^{1/2}$ numbers were obtained either by working in high viscosity mediums where the Schmidt number is large or by working at high flow rates. In the present experiment, only aqueous solutions were used since the focus of this research was aimed toward the field of separation science. This factor limits the Schmidt number to approximately 500. Moreover, the flow rates in this study, as mentioned earlier, were much lower than previously reported since the focus was the application to small scale separations. In the data presented here, large $DnSc^{1/2}$ values were obtained by decreasing the curvature ratio.

As a result of the lack of an adequate fit with the previously derived formulae, **EQ9** was used as a framework to derive a new empirical relationship to better fit the experimental data. The resulting best-fit equation is:

$$\kappa = 1.27 - 0.517 \log(DnSc^{1/2}) + 0.0759 \log(DnSc^{1/2})^2$$

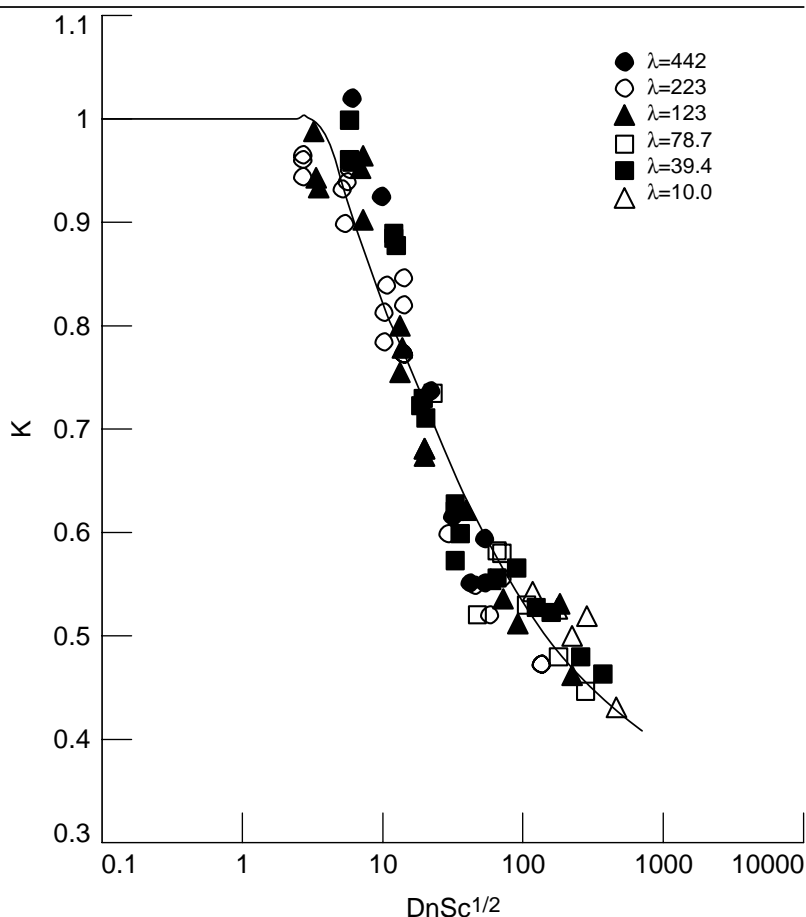
for $DnSc^{1/2} > 4$ and

$$\kappa = 1 \text{ for } DnSc^{1/2} < 4 \quad \text{EQ10}$$

A plot of this relationship with the experimental data is shown in **F8**. Even though there is an appreciable amount of experimental error in the raw data, this new relationship does a good job of predicting the overall trend. From a simple manipulation of this fit, it is possible to predict a curvature ratio for a helically coiled reactor that will give the best performance at a given set of experimental conditions. For example, if tubing with an inner diameter of

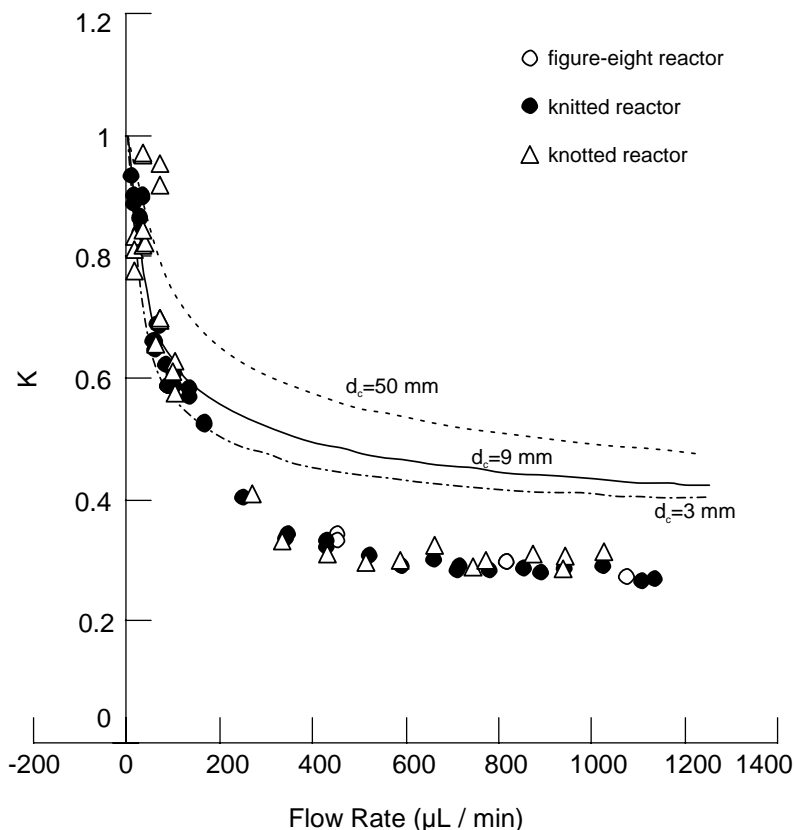
F8

Correlation of dispersion in coiled tubes. Best fit line based on EQ9.



F9

Reduction in dispersion for serpentine reactor geometries, compared to EQ10.



0.225 mm were coiled with a diameter of 2.25 mm, and the flow rate was 0.100 mL/min, the coiled-tube band spreading would be 56% compared to the straight tube case as calculated from EQ10. Therefore, the residence time for the reactor in this case could be 44% larger than in a similar straight tube yielding the same amount of band spreading.

Another method which has been shown to reduce the amount of band spreading in open tubes is performed by deforming the longitudinal flow path in straight tubes to a greater extent than can be accomplished by helical coiling alone. This “serpentine” geometry does not allow the radial flow pattern to fully develop. Instead, it forces the radial streamlines to continually re-orient themselves parallel to the axis of curvature, thereby creating greater radial mixing. Due to the increased complexity of the fluid dynamics in this case, it is very difficult to mathematically predict dispersion values. Therefore, in order to evaluate this technique at microbore flow rates, three different geometries were experimentally studied: a knitted reactor similar to the one discussed by Engelhardt and Neue (21), a knotted reactor of the style developed by Krull, et al. (22), and a simple figure-eight geometry. The construction of each of these is described previously in the experimental section.

The experimental dispersion in these reactors was normalized to the fit for dispersion in the straight reactor as was previously done in the case of the coiled tube data. These values are plotted as a function of the volumetric flow rate in F9. The best-fit results from EQ10 for coiled reactors is also shown for several coil diameters. As this graph demonstrates, it appears that there is very little difference in performance among the three different serpentine reactor geometries. Also, there is little, if any, benefit to the serpentine geometry over the tight

helical coil geometry below flow rates of approximately 0.2 mL/min in these particular reactors. This finding is probably a result of the small radial velocity component at these low axial velocities. However, it should be noted that the actual radius of the bends in the serpentine reactors is approximately twice as large as the 3 mm radius coil depicted in **F9**, thus leading to the conclusion that serpentine geometry enhances the radial mixing better than the helically coiled reactors even at low flow rates.

Conclusion

Both helically coiled and serpentine geometry open-tubular reactors efficiently reduce band spreading at the flow rates studied. However, at microbore flow rates, there seems to be no distinction among the performances of any of the serpentine designs from the 3 mm coil shown in **F9**. The choice

of a reactor for any specific application would depend not only on the band-spreading concerns addressed herein but also on the geometrical needs of the system. In many cases, a cylindrical lamp is used to irradiate the reactor. In such a situation, the knitted reactor may be the best choice as it can be designed to just fit over the lamp, and much of the tubing is in a single layer for better optical transmission.

References

1. W. Iwaoka and S.R. Tannenbaum, *IARC Sci. Publ.* 14 (1976) 51.
2. G. Taylor, *Proc. Roy. Soc. A* 223 (1954) 473.
3. J. Thomson, *Proc. Roy. Soc. A* 25 (1876) 5.
4. J. Thomson, *Proc. Roy. Soc. A* 26 (1877) 356.
5. J.H. Grindley and A.H. Gibson, *Proc. Roy. Soc. A* 80 (1908) 114.
6. J. Eustice, *Proc. Roy. Soc. A* 84 (1910) 107.
7. J. Eustice, *Proc. Roy. Soc. A* 85(1911) 119.
8. G.S. Williams, C.W. Hubell, and G.H. Finkell, *Trans. ASCE* 47 (1902) 7.
9. W.R. Dean, *Phil. Mag.* 28 (1927) 208.
10. W.R. Dean, *Phil. Mag.* 30 (1928) 673.
11. D.M. Ruthven, *Chem. Eng. Sci.* 26 (1971) 1113.
12. R. Aris, *Proc. Roy. Soc. A* 235, (1956) 67.
13. M.E. Erdogan and P. C. Chatwin, *J. Fluid Mech.* 29 (1967) 465.
14. L.A.M. Janssen, *Chem. Eng. Sci.* 31 (1976) 215.
15. V.D. Shetty and K. Vasudeva, *Chem. Eng. Sci.* 32 (1977) 783.
16. E. van Andel, H. Kramers, and A. De Voogd, *Chem. Eng. Sci.* 19 (1964) 77.
17. R.N. Trivedi and K. Vasudeva, *Chem. Eng. Sci.* 30 (1975) 317.
18. K.D.P. Nigam and K. Vasudeva, *Chem. Eng. Sci.* 31 (1976) 835.
19. R.S. Deelder, M.G.F. Kroll, A. J. B. Beeren, and J.H.M. van den Berg, *J. Chromatogr.* 149 (1978) 669.
20. R.N. Iyer and K. Vasudeva, *Chem. Eng. Sci.* 36 (1981) 1104.
21. H. Engelhardt and U.D. Neue, *Chromatographia* 15 (1982) 403.
22. C.M. Selavka, K.S. Jiao, and I.S. Krull, *Anal. Chem.* 59 (1987) 2221.